# REPORT DOCUMENTATION PAGE

*Form Approved OMB No. 0704-0188*



| 1. REPORT DATE *(DD-MM-YYYY)* | 2. REPORT TYPE | 3. DATES COVERED *(From - To)* |
|---|---|---|
| 30-11-2009 | REPRINT | |

**4. TITLE AND SUBTITLE**
On the accuracy of thermionic electron emission models. I. Electron detachment from $SF_6^-$

**5a. CONTRACT NUMBER**

**5b. GRANT NUMBER**

**5c. PROGRAM ELEMENT NUMBER**
61102F

**6. AUTHOR(S)**
Troe, J.*, T.M. Miller, and A.A. Viggiano

**5d. PROJECT NUMBER**
2303

**5e. TASK NUMBER**
HP

**5f. WORK UNIT NUMBER**
A1

**7. PERFORMING ORGANIZATION NAME(S) AND ADDRESS(ES)**

Air Force Research Laboratory
29 Randolph Road
Hanscom AFB MA 01731-3010

**8. PERFORMING ORGANIZATION REPORT NUMBER**

AFRL-RV-HA-TR-2009-1115

**9. SPONSORING / MONITORING AGENCY NAME(S) AND ADDRESS(ES)**

**10. SPONSOR/MONITOR'S ACRONYM(S)**



**12. DISTRIBUTION / AVAILABILITY STATEMENT**
Approved for Public Release; Distribution U.

**13. SUPPLEMENTARY NOTES**
REPRINTED FROM: J. CHEM. PHYS., V. 130, 244303 (2009) 
*Universitat Gottingen, Gottingen, Germany

**14. ABSTRACT**

Detailed statistical rate calculations combined with electron capture theory and kinetic modeling for the electron attachment to $SF_6$ and detachment from $SF_6^-$ [Troe *et al.*, J. Chem. Phys. **127**, 244303 (2007)] are used to test thermionic electron emission models. A new method to calculate the specific detachment rate constants $k_{det}(E)$ and the electron energy distributions $f(E,\varepsilon)$ as functions of the total energy $E$ of the anion and the energy $\varepsilon$ of the emitted electrons is presented, which is computationally simple but neglects fine structures in the detailed $k_{det}(E)$. Reduced electron energy distributions $f(E,\varepsilon/\langle\varepsilon\rangle)$ were found to be of the form $(\varepsilon/\langle\varepsilon\rangle)^n \exp(-\varepsilon/\langle\varepsilon\rangle)$ with $n \approx 0.15$, whose shape corresponds to thermal distributions only to a limited extent. In contrast, the average energies $\langle\varepsilon(E)\rangle$ can be roughly estimated within thermionic emission and finite heat bath concepts. An effective temperature $T_d(E)$ is determined from the relation $E-EA=\langle E_{SF_6}(T_d)\rangle+kT_d$, where $\langle E_{SF_6}(T_d)\rangle$ denotes the thermal internal energy of the detachment product $SF_6$ at the temperature $T_d$ and EA is the electron affinity of $SF_6$. The average electron energy is then approximately given by $\langle\varepsilon(E)\rangle=kT_d(E)$, but dynamical details of the process are not accounted for by this approach. Simplified representations of $k_{det}(E)$ in terms of $T_d(E)$ from the literature are shown to lead to only semiquantitative agreement with the equally simple but more accurate calculations presented here. An effective "isokinetic" electron emission temperature $T_e(E)$ does not appear to be useful for the electron detachment system considered because it neither provides advantages over a representation of $k_{det}(E)$ as a function of $T_d(E)$, nor are recommended relations between $T_e(E)$ and $T_d(E)$ of sufficient accuracy. © *2009 American Institute of Physics*. [DOI: 10.1063/1.3149782]

**15. SUBJECT TERMS**
Sulfur hexafluoride Electron attachment Thermionic emission

| 16. SECURITY CLASSIFICATION OF: | | | 17. LIMITATION OF ABSTRACT | 18. NUMBER OF PAGES | 19a. NAME OF RESPONSIBLE PERSON |
|---|---|---|---|---|---|
| a. REPORT | b. ABSTRACT | c. THIS PAGE | SAR | | A.A. Viggiano |
| UNCLAS | UNCLAS | UNCLAS | | | 19b. TELEPHONE NUMBER *(include area code)* |

THE JOURNAL OF CHEMICAL PHYSICS 130, 244303 (2009)

# On the accuracy of thermionic electron emission models. I. Electron detachment from $SF_6^-$

Jürgen Troe,[1,a] Thomas M. Miller,[2] and Albert A. Viggiano[2]
[1]*Institut für Physikalische Chemie, Universität Göttingen, Tammannstrasse 6, D-37077 Göttingen, Germany and Max-Planck-Institut für Biophysikalische Chemie, D-37077 Göttingen, Germany*
[2]*Air Force Research Laboratory, Space Vehicles Directorate, Hanscom Air Force Base, Bedford, Massachusetts 01731-3010, USA*

(Received 10 March 2009; accepted 14 May 2009; published online 24 June 2009)



Detailed statistical rate calculations combined with electron capture theory and kinetic modeling for the electron attachment to $SF_6$ and detachment from $SF_6^-$ [Troe *et al.*, J. Chem. Phys. **127**, 244303 (2007)] are used to test thermionic electron emission models. A new method to calculate the specific detachment rate constants $k_{det}(E)$ and the electron energy distributions $f(E,\varepsilon)$ as functions of the total energy $E$ of the anion and the energy $\varepsilon$ of the emitted electrons is presented, which is computationally simple but neglects fine structures in the detailed $k_{det}(E)$. Reduced electron energy distributions $f(E,\varepsilon/\langle\varepsilon\rangle)$ were found to be of the form $(\varepsilon/\langle\varepsilon\rangle)^n \exp(-\varepsilon/\langle\varepsilon\rangle)$ with $n\approx 0.15$, whose shape corresponds to thermal distributions only to a limited extent. In contrast, the average energies $\langle\varepsilon(E)\rangle$ can be roughly estimated within thermionic emission and finite heat bath concepts. An effective temperature $T_d(E)$ is determined from the relation $E-\mathrm{EA}=\langle E_{SF_6}(T_d)\rangle+kT_d$, where $\langle E_{SF_6}(T_d)\rangle$ denotes the thermal internal energy of the detachment product $SF_6$ at the temperature $T_d$ and EA is the electron affinity of $SF_6$. The average electron energy is then approximately given by $\langle\varepsilon(E)\rangle=kT_d(E)$, but dynamical details of the process are not accounted for by this approach. Simplified representations of $k_{det}(E)$ in terms of $T_d(E)$ from the literature are shown to lead to only semiquantitative agreement with the equally simple but more accurate calculations presented here. An effective "isokinetic" electron emission temperature $T_e(E)$ does not appear to be useful for the electron detachment system considered because it neither provides advantages over a representation of $k_{det}(E)$ as a function of $T_d(E)$, nor are recommended relations between $T_e(E)$ and $T_d(E)$ of sufficient accuracy. © *2009 American Institute of Physics*. [DOI: 10.1063/1.3149782]

## I. INTRODUCTION

Molecular systems with several internal degrees of freedom often act as their own heat bath. In this picture, the fixed microcanonical internal energy $E$ is distributed over the internal degrees of freedom in a quasithermal manner and often it is expedient to define an effective temperature $T$ through the relation

$$\langle E(T)\rangle = E, \tag{1.1}$$

$\langle E(T)\rangle$ here denotes the average thermal internal energy of the molecules in a canonical ensemble at the temperature $T$. In other words, an effective temperature $T$ is defined such that the average energy $\langle E(T)\rangle$ in a canonical ensemble equals the microcanonical energy $E$.

Equation (1.1) allows one to compare physical properties $Y$ of the molecular system in microcanonical and canonical ensembles. Some properties depend on the internal energy distribution in such a way that $Y(E)$ and $Y(T)$ approach each other provided that a valid relation (1.1) is fulfilled. For instance, it has been demonstrated both experimentally[1] and theoretically[2,3] that UV absorption cross sections $\sigma(\lambda)$ of vibrationally excited polyatomic molecules in microcanonical and canonical ensembles are practically the same when $\sigma(\lambda,E)$ and $\sigma(\lambda,T)$ are compared and Eq. (1.1) is obeyed. The situation may change when product energy distributions of bond fission processes are considered. As a consequence of the heat bath concept, one would expect quasithermal distributions of product translations, rotations, and vibrations which all correspond to the same temperature, see, e.g. Ref. 4. However, dynamical effects often are found to produce differences between the respective effective temperatures, see, e.g., the calculations for the fragmentation of *n*-propyl benzene cations in Ref. 5. The concept finally loses its significance when the physical property $Y$ samples the high-energy tail of the internal energy distribution. In canonical ensembles the energies extend to high values, whereas they are restrained by the value of $E$ in microcanonical ensembles. Correspondingly, specific rate constants $k(E)$ and their thermal analogs $k(T)$ of processes with large threshold energies, in general, cannot be related by means of Eq. (1.1).

The present article deals with a phenomenon which has been also analyzed in terms of the heat bath concept, i.e., the detachment of electrons from metastable molecular anions or negatively charged clusters. The phenomenon has been termed "thermionic electron emission;" for an extensive review see, e.g., Ref. 6. Once again the question arises as to

[a]Author to whom correspondence should be addressed. Electronic mail: shoff@gwdg.de.

 

how far the heat bath concept holds or to what extent dynamical effects require modifications. This is the subject of the present article.

We base our analysis of electron detachment (or "emission") rates on a theoretical treatment of the detachment dynamics by statistical unimolecular rate theory combined with electron capture theory. In addition, specific kinetic effects of the considered system, which influence the attachment/detachment process, are accounted for. An essential element of the treatment is the link between the lifetimes of the excited anions with respect to electron detachment and the cross sections for the corresponding electron attachment. This link is provided by detailed balancing. It is automatically included in statistical rate theory and it is common to most thermionic emission models, see, e.g., Ref. 6. A necessary condition for the application of detailed balancing, however, is that the linked processes are truly reverse. This aspect will also be examined in the present article.

Within a finite heat bath concept, effective temperatures of the parent anions, the daughter neutrals and the emitted electrons have been formulated in a number of ways.[6–10] These, however, are not necessarily consistent with Eq. (1.1). As the characterization of electron attachment and detachment has made progress over the last years, it appears useful to reconsider these effective temperatures and to investigate the influence of dynamic factors.

It is clear that the definition of an effective electron emission temperature at low electron energies meets with problems. For illustration we consider a process of the type

$$A^{-*} \rightarrow A + e^- \tag{1.2}$$

at an energy $E$ of the excited parent anion $A^{-*}$ which is not much larger than the threshold energy of the process. The latter is assumed to be given by the electron affinity (EA) of A. If the energy $E-EA$ available to the electron is smaller than the energy of the first vibrationally excited state of the daughter neutral A, there is no multilevel heat bath of A over which the energy $E-EA$ could be distributed. Instead the electron energy $\varepsilon$ is fixed and given by the difference $\varepsilon = E - EA$, whereas the internal energy of A, $E-EA-\varepsilon$, is zero. Although Eq. (1.1) could be applied to this situation as well, the derived temperature would have only little in common with that of a heat bath. On the other hand, if $E-EA$ reaches up into the vibrational quasicontinuum of A, there will be broad distributions of electron energies, finite heat bath models might be considered, and an effective electron temperature could be defined more meaningfully. Two questions arise: At which energies $E-EA$ does the transition from low- to high-energy behavior occur, and how are effective temperatures related to the kinetic and dynamic details of the process (1.2). We focus attention on these questions in the present article for a number of reasons. First, we feel that the statistical theory of electron attachment/detachment processes in the framework of thermionic emission models[6] often has been used in an oversimplified manner. Second, we recently have extended[11,12] Vogt–Wannier[13] (VW) and Fabrikant–Hotop-type[14] capture theory for electron attachment. The results of this work may be implemented into statistical calculations of electron detachment rates. Third, we have provided a detailed kinetic modelling[15,16] of the mechanism of low-energy electron attachment to $SF_6$ and the corresponding electron detachment from $SF_6^-$,

$$SF_6^- \Leftrightarrow SF_6 + e^-. \tag{1.3}$$

This model is "user friendly," it can easily be generalized to other attachment/detachment systems, and it can incorporate specific dynamical and kinetic factors for individual reactions. For reaction (1.3), e.g., it was suggested that the experimental cross sections for nondissociative electron attachment include kinetic factors which account for electron capture into a virtual state $e^-SF_6$, "intramolecular vibrational redistribution" (IVR) (or electron-phonon coupling) leading from $e^-SF_6$ to anionic $SF_6^{-*}$, and inelastic vibrational excitation (VEX) of $SF_6$ in competition with IVR from $e^-SF_6$ to $SF_6^{-*}$. VEX can either proceed through highly excited anionic $SF_6^{-*}$ or it can avoid the intermediate formation of metastable $SF_6^{-*}$. Alternative, yet more complicated, descriptions of the attachment process in terms of Gauyacq–Herzenberg resonance theory[14,17,18] have also been elaborated and might be compared with VW-type electron capture theory.[11–14] Finally, our recent measurements of thermal attachment and detachment rates[19] through a third law analysis of the equilibrium constant led to a revised value of the EA of $SF_6$, suggested to be $EA(SF_6) = 1.20(\pm 0.05)$ eV. This, in turn, gave rise to a revision of statistical calculations of the specific rate constants $k_{det}(E)$ for electron detachment from $SF_6^{-*}$ and of the lifetimes $1/k_{det}(E)$ of $SF_6^{-*}$.

Because of the wealth of theoretical and experimental studies available for the $SF_6^-$ system, it appears attractive to inspect thermionic electron emission models for reaction (1.3). This is even more timely since storage ring measurements[20] of $SF_6^-$ lifetimes have recently been evaluated in terms of such models,[21] the latter analysis suggesting a value of $EA(SF_6) = 1.4$ eV, which is higher than the value of EA = 1.20 eV derived in Ref. 19. The present article inspects electron detachment rates from $SF_6^-$ over a wide energy range, employing electron capture theory combined with statistical rate theory without the simplifications usually made in thermionic emission models.[6] It also traces the reasons for the discrepancy between the $EA(SF_6)$ values suggested in Refs. 19 and 21. Attention in our work is finally paid to the transition from low- to high-energy behavior. With the experience gained for the $SF_6^-$ system, the treatment may be extended to larger species such as $C_{60}^-$ or other negatively charged atomic clusters. This continuation of our work will be presented in future publications.

Before elaborating the theory of electron energy distributions and detachment rates, one particular remark about the relation between cross sections for nondissociative electron attachment to $SF_6$ and detachment rate constants should be made. It was suggested in Ref. 15 that the experimental attachment cross sections to $SF_6$ contain contributions from several kinetic processes such as primary electron capture, IVR, and VEX. The question arises which of these contributions, through detailed balancing, should be included in calculations of detachment rate constants $k_{det}(E)$. Therefore, $k_{det}(E)$ in Ref. 15 was calculated alternatively with and with-

out the individual kinetic factors. This is an important kinetic aspect of the problem which should be taken into account in all systems for which thermionic emission models are applied. We will readdress this point later.

## II. STATISTICAL RATE THEORY

In the following we briefly summarize the basic equations of statistical unimolecular rate theory[4] such as they were adapted in our recent work to electron detachment/attachment processes.[15] The starting point is the specific rate constant for detachment,

$$k_{\mathrm{det}}(E,J) = W_{\mathrm{det}}(E,J)/h\rho_p(E,J) \tag{2.1}$$

at the energy $E$ and total angular momentum $J$, with Planck's constant $h$, the "number of open reaction channels" or the "cumulative reaction probability" $W_{\mathrm{det}}(E,J)$, and the rovibrational density of states of the parent anion $\rho_p(E,J)$. One may, or may not, include in $W_{\mathrm{det}}(E,J)$ the electronic degeneracy factor of 2, originating from the spin of the emitted electron because the same factor, now originating from the doublet of the anion, is contained in $\rho_p(E,J)$. These factors cancel in Eq. (2.1). It appears confusing to explicitly account for this factor in $W_{\mathrm{det}}(E,J)$ and to leave it implicitly in $\rho_p(E,J)$. Since they cancel, in the present work the electronic degeneracies are omitted from the beginning both from $W_{\mathrm{det}}(E,J)$ and $\rho_p(E,J)$.

$W_{\mathrm{det}}(E,J)$ is given by

$$W_{\mathrm{det}}(E,J) = \sum_i P(E-E_{0i}), \tag{2.2}$$

where the $E_{0i}$ are the energy levels of the daughter neutral species and $P(E-E_{0i})$ are the transmission coefficients for the outgoing (in detachment) or incoming (in attachment) electrons. Because of microscopic reversibility, the latter are the same under the condition that the same dynamical phenomena are compared. The cross sections for attachment, starting from the level $E_{0i}$, then are directly related to the detachment rate constants through detailed balancing, i.e., through the relationship

$$\sigma(k_i) = (\pi/k_{pi}^2)\sum_{l=0}^{\infty}(2l+1)P_l(k_{pi}), \tag{2.3}$$

where $k_{pi}=p_i/\hbar=\sqrt{2\mu(E-E_{0i})}/\hbar$ and

$$P(E-E_{0i}) = \sum_{l=0}^{\infty}(2l+1)P_l(k_{pi}). \tag{2.4}$$

Above, $k_{pi}$ is the wavenumber for momentum $p_i$ and $\mu$ is the reduced mass of $SF_6$ and $e^-$. If only $s$-waves need to be considered, such as in the electron detachment/attachment of $SF_6^-$, one has $P(E-E_{0i})=P_{l=0}(k_{pi})$. This property of the $SF_6^-$ system very much simplifies the treatment. If higher waves are included, their angular momentum (quantum number $l$) contributes to the total angular momentum (quantum number $J$) which needs particular attention when Eqs. (2.3) and (2.4) are combined with Eq. (2.2).

Electron capture or resonance theories[11–15] provide suitable expressions for the $P_l(k_{pi})$, both for the case of daughter neutrals having induced or having permanent dipole moments.[12] The study of the $SF_6^-$ system in Ref. 15 suggested that the mechanistic complications arising from IVR and inelastic VEX can empirically be accounted for by factors to be multiplied with the $P_l(k_{pi})$. Below we inspect the consequences of such effects for electron emission properties.

For each reaction channel $i$, the energy of the electrons $\varepsilon_i$ is equal to the energy difference $E-E_{0i}$, i.e.,

$$\varepsilon_i = E - E_{0i}. \tag{2.5}$$

In the following, we are interested in partial specific rate constants $k_{\mathrm{det}}(E,\varepsilon_i)$ for electron detachment. As long as only one channel $E_{0i}$ is open, i.e., $E_{0i}$=EA, one has $\varepsilon_i=\varepsilon=E-\mathrm{EA}$ and $k_{\mathrm{det}}(E,\varepsilon_i)$ is given by

$$k_{\mathrm{det}}(E,\varepsilon_i) = k_{\mathrm{det}}(E,\varepsilon) = P(\varepsilon)/h\rho_p(E). \tag{2.6}$$

[In the following we omit the $J$-dependence which was elaborated in Ref. 15 and only consider $k_{\mathrm{det}}(E,J=0)$ which we denote by $k_{\mathrm{det}}(E)$. However, we note that, for $s$-wave scattering, one has $J=j$, where $j$ corresponds to the total angular momentum of the neutral daughter. In principle, all $k_{\mathrm{det}}(E,J)$ need to be considered, see Ref. 15]. In the low-energy region there is no difference between partial, $k_{\mathrm{det}}(E,\varepsilon)$, and total, $k_{\mathrm{det}}(E)$, detachment rate constants. Increasing the energy into the sparse manifold of the daughter vibrational levels $E_{0i}$, at a given total energy $E$ there are several levels $i$ with electron energies $\varepsilon_i$ which contribute, and one has

$$k_{\mathrm{det}}(E) = \sum_i k_{\mathrm{det}}(E,\varepsilon_i), \tag{2.7}$$

with

$$k_{\mathrm{det}}(E,\varepsilon_i) = P(\varepsilon_i)/h\rho_p(E). \tag{2.8}$$

In this case one will have a discrete distribution $F(E,\varepsilon_i)$ of electron energies defined by

$$F(E,\varepsilon_i) = k_{\mathrm{det}}(E,\varepsilon_i)/k_{\mathrm{det}}(E) = P(\varepsilon_i)\Big/\sum_i P(\varepsilon_i). \tag{2.9}$$

Further increasing the energy into the vibrational quasicontinuum of the daughter states, one switches to a quasicontinuous distribution function $f(E,\varepsilon)$ of electron detachment rate constants defined by

$$f(E,\varepsilon) = k_{\mathrm{det}}(E,\varepsilon)/k_{\mathrm{det}}(E). \tag{2.10}$$

In this case, the summation over $i$ in $k_{\mathrm{det}}(E)$ is replaced by an integral over $\varepsilon$ weighted by the vibrational density of states $\rho_d(E-\mathrm{EA}-\varepsilon)$ of the daughter neutral. The combination of Eqs. (2.1)–(2.5) then leads to the partial rate constant per energy $\varepsilon$ interval,

$$k_{\mathrm{det}}(E,\varepsilon) = \frac{\mu\rho_d(E-\mathrm{EA}-\varepsilon)\sigma(\varepsilon)\varepsilon}{\pi^2\hbar^3\rho_p(E)}, \tag{2.11}$$

and, hence, to the distribution function per energy interval,

$$f(E,\varepsilon) = \frac{\sigma(\varepsilon)\varepsilon\rho_d(E-\mathrm{EA}-\varepsilon)}{\int_0^{E-\mathrm{EA}}\sigma(\varepsilon)\varepsilon\rho_d(E-\mathrm{EA}-\varepsilon)d\varepsilon}. \quad (2.12)$$

Equation (2.11) agrees with the general formulation in Ref. 6. However, one should note again that in the present work $\rho_d$ and $\rho_p$ both are pure vibrational densities of states and the cancelling electronic degeneracies have been taken care of separately. [The factor of 2 in the numerator of Eq. (2) of Ref. 6 then disappears, see above.] In addition, $k_{\mathrm{det}}(E)$, $f(E,\varepsilon)$, and $\sigma(\varepsilon)$ should correspond to the same dynamical and kinetic process in the forward and reverse directions. This caveat is important to be kept in mind.

In the following, we explicitly determine $k_{\mathrm{det}}(E)$, $F(E,\varepsilon_i)$, and $f(E,\varepsilon)$ for electron detachment from $SF_6^-$ and, we analyze the contributions of the various kinetic factors to these quantities. We base our calculations on the molecular parameters of $SF_6^-$ and $SF_6$ from Ref. 22, such as given in Appendix and also employed in Ref. 15.

## III. DETACHMENT RATES AND ELECTRON ENERGY DISTRIBUTIONS FROM $SF_6^-$

Total specific rate constants $k_{\mathrm{det}}(E,J)$ for electron detachment from $SF_6^-$ in Ref. 15 were calculated in detail and documented over the range $E=1.2-2.2$ eV. The results showed a considerable fine structure caused by the sparse character of the vibrational manifold of the $E_{0i}$ of $SF_6$. The $J$-dependence was also illustrated over the range for $J=0-200$. Calculations were compared employing (i) $P(E-E_{0i})=1$ at $E\geq E_{0i}$ [and $P(E-E_{0i})=0$ at $E<E_{0i}$], (ii) $P(E-E_{0i})$ from pure electron capture theory, and (iii) $P(E-E_{0i})$ including kinetic factors arising from IVR and VEX. In the following, we analyze the corresponding $k_{\mathrm{det}}(E)$ and the energy distribution of the emitted electrons, alternatively including or omitting the kinetic factors.

In our analysis we follow the approach outlined in Ref. 15. We start with the "Rice–Ramsperger–Kassel–Marcus (RRKM)-type" treatment where the $P(E-E_{0i})$ are step functions rising from zero to unity at all individual $E\geq E_{0i}$. We then continue with pure electron capture theory, improving Klots' analytical approximation[23] to $P(E-E_{0i})$ for s-wave capture within the VW model, using the expression derived in Ref. 12,

$$P(E-E_{0i}) = P^{\mathrm{VW}}(E-E_{0i}) \approx 1-0.5\exp(-2\kappa_i)-0.5\exp(-6\kappa_i), \quad (3.1)$$

with

$$\kappa_i = \mu e\sqrt{2\alpha(E-E_{0i})}/\hbar^2. \quad (3.2)$$

Here, $e$ notes the electronic charge and $\alpha$ is the isotropic polarizability of $SF_6$, taken as $\alpha=6.54\times10^{-24}$ cm$^3$. This leads to the reduced energy scale $\kappa_i=1.80[(E-E_{0i})/\mathrm{eV}]^{1/2}$. Suggesting[15] that both the experimental nondissociative attachment cross sections[24–26] and the thermal detachment rate constants[15,27,28] for $SF_6^-$ are not only determined by pure electron capture but also include contributions from IVR, we then modify $P(\kappa_i)$ by an additional, empirical, factor $P^{\mathrm{IVR}}(\kappa_i)$. In Ref. 15 this factor was assumed to have the form

$$P^{\mathrm{IVR}}(\kappa_i) \approx \exp(-c_1\kappa_i^2). \quad (3.3)$$

The analysis of experimental thermal attachment rate constants between 50 and 700 K led to a temperature dependent fit parameter, being $c_1\approx1.92$ for 300 K. While the parameter $c_1$ is still quite uncertain for the range of 50–200 K, its value appears well established for 200–700 K, see the analysis in Ref. 15. It should nevertheless be emphasized that the kinetic factor of Eq. (3.3), as suggested by the analysis of thermal attachment rate constants, is based on information for a limited energy range only. One, therefore, cannot expect that Eq. (3.3) applies to larger energy ranges. We keep this restriction in mind when larger energy ranges are considered. [Equation (3.3) may also include contributions from an energy dependence of the effective polarizability of $SF_6$ which is not further considered here.]

The analysis of experimental nondissociative attachment cross sections suggested that yet another dynamical factor should be included in $P(\kappa_i)$ for attachment which accounts for inelastic collisions between $e^-$ and $SF_6$ without $SF_6^{-*}$ being formed. This factor was suggested[15] to be of the form $P^{\mathrm{VEX}}=1$ for $\kappa_i\leq\kappa_{\nu_1}$ and

$$P^{\mathrm{VEX}}(\kappa_i) \approx \exp[-c_2(\kappa_i^2-\kappa_{\nu_1}^2)] \quad (3.4)$$

for $\kappa_i\geq\kappa_{\nu_1}$, where $\kappa_{\nu_1}=0.588$ corresponds to an energy $E-\mathrm{EA}$ of 0.096 eV and $c_2$ empirically was fitted as $c_2\approx6.0$ for 300 K. If this assumption of competing electron attachment forming $SF_6^{-*}$ and inelastic electron scattering avoiding $SF_6^{-*}$ is correct, then $P^{\mathrm{VEX}}(\kappa_i)$ should be included in the overall nondissociative attachment cross sections, but it should not be included in the detachment rate constants. On the other hand, $P^{\mathrm{IVR}}(\kappa_i)$ should be included in the detachment rate constants because detachment also invokes IVR. As this interpretation, however, is still uncertain, $k_{\mathrm{det}}(E)$ in Ref. 15 alternatively was calculated with and without the factor $P^{\mathrm{VEX}}(\kappa_i)$. In the following, we omit the $P^{\mathrm{VEX}}(\kappa_i)$ factor, assuming that the described mechanism is correct. We emphasize that experimental nondissociative attachment cross sections and detachment rate constants then are not directly linked by detailed balancing because they only partly correspond to reverse kinetics. [In Refs. 15 and 16 $P^{\mathrm{IVR}}(\kappa_i)$ and $P^{\mathrm{VEX}}(\kappa_i)$ could be separated only up to an energy of about $E-E_0\approx0.2$ eV, while for larger energies up to about $E-E_0\approx2$ eV, only the product of the two factors was fitted to the experimental total attachment cross sections; a separation of the two factors at large energies was not possible. This limits the possibilities to design $k_{\mathrm{det}}(E)$. It is even not proven that the differences between experimentally observed thermal nondissociative attachment rate coefficients at temperatures below about 700 K and calculations with the VW electron capture model[15] are due to IVR or as well to VEX. In the latter case, $k_{\mathrm{det}}(E)$ would only contain VW contributions.] In spite of the remaining interpretational uncertainties, Eqs. (2.3), (2.4), and (3.1)–(3.4) in Refs. 15 and 16 were shown to provide a very good representation of the available experimental attachment cross sections and thermal attachment rate coefficients [both $k_{\mathrm{at}}(T_{\mathrm{gas}}=T_{\mathrm{el}})$ and $k_{\mathrm{at}}(T_{\mathrm{gas}}\neq T_{\mathrm{el}})$].

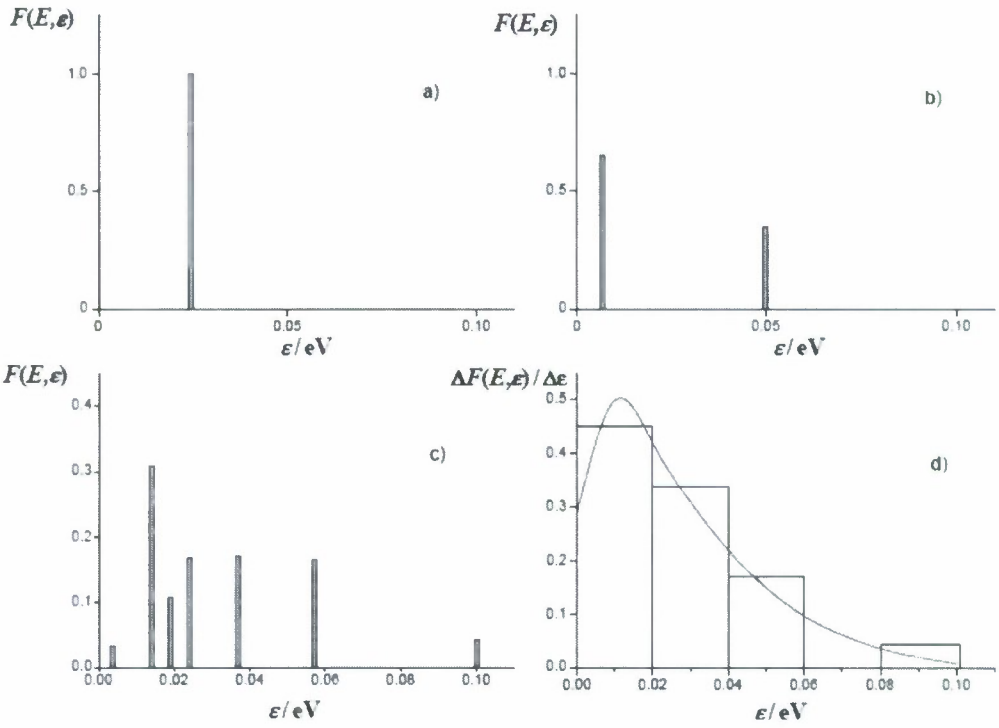


FIG. 1. Discrete distributions $F(E,\varepsilon)$ of electron energies $\varepsilon$ in the detachment from $SF_6^-$ at the energies $E-EA=0.025$ eV (a), 0.05 eV (b), and 0.1 eV [(c) and (d)]. (d) shows $\Delta F(E,\varepsilon)/\Delta\varepsilon$ with bins $\Delta\varepsilon=0.02$ eV; the continuous curve is from Eq. (2.12), see text.

With the given expressions, specific rate constants $k_{det}(E)$ as well as the distributions $F(E,\varepsilon_i)$ and $f(E,\varepsilon)$ of the electron energies defined in Eqs. (2.9) and (2.10) can directly be calculated. First, at energies $E-EA=\varepsilon\leq 0.0429$ eV (corresponding to the first excited vibrational state of $SF_6$ at $E_{0i}=0.0429$ eV$=hc$ 346 cm$^{-1}$), one has

$$F(\varepsilon)=1. \tag{3.5}$$

Equation (3.5) corresponds to the range where only a single channel is open. Second, in the range of the sparse manifold of vibrational levels of $SF_6$, the contributions from individual channels[15] $E_{0i}$ are easily summed up individually. Figure 1 shows examples for three values of $E-EA$ in the range of 0–0.1 eV. As $P^{VEX}(\kappa_i)=1$ over the range of 0–0.096 eV, the question of including or excluding $P^{VEX}(\kappa_i)$ practically does not arise here. Figure 1 well illustrates the discrete nature of $F(E,\varepsilon_i)$ which has its equivalent in the marked fine structure of the calculated $k_{det}(E)$, see below.

Moving up to higher energies, into the vibrational quasicontinuum of $SF_6$, the distribution function $f(E,\varepsilon)$ of Eq. (2.10) with Eq. (2.12) takes the form

$$f(E,\varepsilon)=\frac{P(E,\varepsilon)\rho_d(E-EA-\varepsilon)}{\int_0^{E-EA}P(E,\varepsilon)\rho_d(E-EA-\varepsilon)d\varepsilon}. \tag{3.6}$$

The use of Eq. (3.6) requires a smoothed expression for the density of states $\rho_d(E')$. Most conveniently this is obtained from the Whitten–Rabinovitch approximation,[4]

$$\rho_d(E')\simeq\frac{[E'+a(E')E_z]^{s-1}}{(s-1)!\Pi_{i=1}^{s}h\nu_i}, \tag{3.7}$$

where $h\nu_i$ are the $s$ vibrational quanta and $E_z=1/2\Sigma_{i=1}^{s}h\nu_i$ is the vibrational zero point energy of $SF_6$. The Whitten–Rabinovitch correction function $a(E')$ is given by[4]

$$a(E')=1-\beta\omega, \tag{3.8a}$$

with

$$\log_{10}\omega\approx-1.0506(E'/E_z)^{0.25}\quad\text{at } E'>E_z, \tag{3.8b}$$

$$\omega^{-1}\approx 5(E'/E_z)+2.73(E'/E_z)^{0.5}+3.51\quad\text{at } E'<E_z \tag{3.8c}$$

and

$$\beta=(s-1)^2\sum_{i=1}^{s}(h\nu_i)^2/s\left[\sum_{i=1}^{s}h\nu_i\right]^2. \tag{3.8d}$$

At the high-energy end of $\varepsilon$, i.e., at $\varepsilon\rightarrow E-EA$, $\rho_d(E')$ reaches down into the sparse manifold of vibrational energy levels of $SF_6$. However, $f(\varepsilon)$ markedly decreases with $\varepsilon$ at the high-energy end such that this is not a practical problem. A smooth transition between the continuous $f(\varepsilon)$ and the discrete $\Delta F(\varepsilon_i)/\Delta\varepsilon$ is obtained when Eqs. (3.6), (3.7), (3.8a), (3.8b), (3.8c), and (3.8d) are used. For example, Fig. 1(d) sums the discrete contributions to $F(E,\varepsilon)$ of Fig. 1(c) into bins of width $\Delta\varepsilon=0.02$ eV and compares the corresponding $\Delta F(E,\varepsilon_i)/\Delta\varepsilon$ with $f(E,\varepsilon)$, the latter being calculated with Eqs. (3.6), (3.7), (3.8a), (3.8b), (3.8c), and (3.8d). The ap-

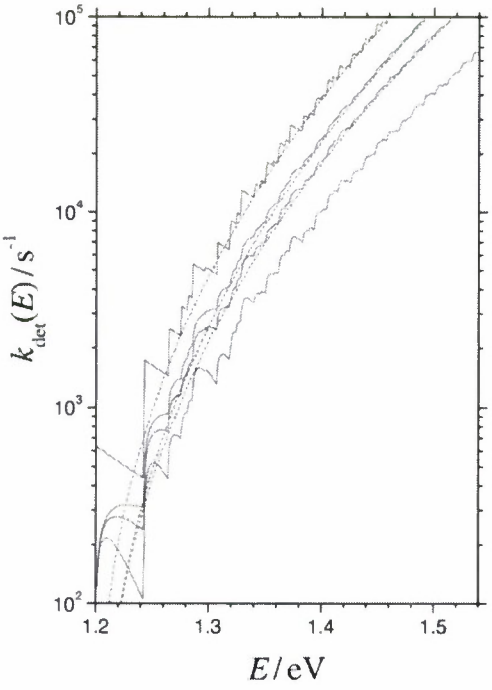


FIG. 2. Specific rate constants $k_{det}(E)$ for electron detachment from $SF_6^-$. Curves from top to bottom: (i) RRKM-type model without electron capture contributions, i.e., $P(E-E_{0i})=1$ for $E>E_{0i}$; (ii) pure electron capture model, i.e., $P(E-E_{0i})=P^{VW}(E-E_{0i})$; (iii) electron capture with IVR contribution, i.e., $P(E-E_{0i})=P^{VW}(E-E_{0i})P^{IVR}(E-E_{0i})$; (iv) electron capture with IVR and VEX contributions, i.e., $P(E-E_{0i})=P^{VW}(E-E_{0i})P^{IVR}(E-E_{0i})P^{VEX}(E-E_{0i})$. Full curves: Detailed calculations from Ref. 15; dashed curves for the upper three models: Simplified calculations with Eq. (3.9) from the present work, see text.

proach of the discrete results by the continuum distribution is well documented.

$k_{det}(E)$ in Ref. 15 with Eqs. (2.1)–(2.4) and (3.1)–(3.4) was calculated without further simplifications. With increasing number of contributing channels $i$ at increasing energy, however, the calculation becomes increasingly cumbersome. The explicit calculation then is considerably simplified when the Whitten–Rabinovitch approximation for the densities of states is employed and $k_{det}(E)$ is derived from the expression

$$k_{det}(E) \approx \int_0^{E-EA} P(E,\varepsilon)\rho_d(E-EA-\varepsilon)d\varepsilon/h\rho_p(E). \quad (3.9)$$

However, one sacrifices the fine structures of $k_{det}(E)$. Figure 2 compares the simplified $k_{det}(E)$ from Eq. (3.9) with detailed results from Ref. 15 such as calculated with discrete channels $i$. Apart from the fine structure the agreement looks very satisfactory. Employing Eqs. (3.7), (3.8a), (3.8b), (3.8c), and (3.8d), there is a minor difference (about 30%) between the simplified and accurate results which reflects the inaccuracy of Eq. (3.8a), (3.8b), (3.8c), and (3.8d) at small energies. In part this is due to the degeneracy of the vibrational frequencies used in the calculations (see Appendix). It is known that the Whitten–Rabinovitch approximation then is less accurate than that is normally the case. One can mostly remove this problem by slightly modifying the Whitten–Rabinovitch parameters $\beta$ in Eq. (3.8d). We have done this by fitting the Whitten–Rabinovitch densities of states for $SF_6$ near $E-EA=0.29(\pm 0.05)$ eV to Beyer–Swinehart counting results.[4] This is achieved by reducing the parameter $\beta$ from Eq. (3.8d) by a factor of 0.907 65. [As $E$ is much larger than $E-EA$, $\rho_p(E)$ needs no such correction.] The inaccuracy of Eq. (3.9) then nearly disappears. Figure 2 compares the corresponding results with three of the detailed calculations from Ref. 15. Figure 2 shows, from top to bottom, $k_{det}(E)$ for (i) the "RRKM-type model" [i.e., $P(E-E_{0i})=1$ for $E \geqslant E_{0i}$], (ii) for the pure electron capture "VW-type model" [i.e., $P(E-E_{0i})=P^{VW}(E-E_{0i})$ from Eq. (3.1)], (iii) for a "VW +IVR-type model" with electron capture followed by IVR [i.e., $P(E-E_{0i})=P^{VW}(E-E_{0i})P^{tVR}(E-E_{0i})$ from Eqs. (3.1)–(3.3)], and (iv) for a "VW+IVR+VEX-type model" with electron capture followed by IVR and competing with VEX [i.e., $P(E-E_{0i})=P^{VW}(E-E_{0i})=P^{IVR}(E-E_{0i})P^{VEX}(E-E_{0i})$ from Eqs. (3.1)–(3.4)].

Having gained confidence in the use of the (slightly corrected) Whitten–Rabinovitch approximation for densities of states in calculations of detachment rate constants $k_{det}(E)$ through Eq. (3.9), we use this approximation also in the calculations of electron energy distributions $f(E,\varepsilon)$ through Eq. (3.6). We first analyze the influence of the various contributions to $P(E,\varepsilon)$ on the shape of the distribution functions. We consider an energy $E-EA=1$ eV which is well above the discrete range characterized in Fig. 1. Figure 3 shows the results. A representation of $f(E,\varepsilon)$ as a function of $\varepsilon$ here is chosen. In comparing the results with statistical unimolecular rate theory[4] one should remember that, unlike normal unimolecular reactions, the present system is characterized by $l=0$ such that $J=j$, see above. In spite of this difference, $f(E,\varepsilon)$ for the RRKM-type model looks similar to product translational energy distributions for fragmentations where one fragment is an atom, see, e.g., Refs. 4 and 29. The maximum of $f(E,\varepsilon)$ then is found near $\varepsilon=0$. The specific dynamical effects of electron detachment, such as given by electron

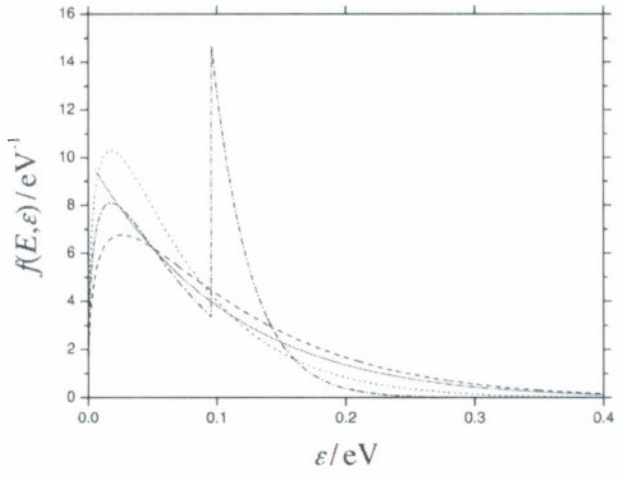


FIG. 3. Energy distribution $f(E,\varepsilon)$ of electrons from the detachment from $SF_6^-$ ($E-EA=1$ eV); full line: RRKM-type model; dashed line: electron capture VW model; dotted line: electron capture with IVR model; dash-dotted line with peak near 0.1 eV: electron capture with IVR and VEX model, see text.

capture theory, IVR, and VEX contributions, change this picture to some extent such as illustrated in Fig. 3. If the experimental attachment cross sections with their marked drop at $\varepsilon > 0.096$ eV would be used for the calculation of $f(E,\varepsilon)$, then one would have a second maximum near $\varepsilon = 0.1$ eV such as shown in the figure. However, as explained above we consider the curve corresponding to electron capture with combined IVR and VEX contributions as being unrealistic, because VEX presumably is not concerned in electron detachment. Therefore, in the following we do not further include the VEX contributions from Eq. (3.4). We also keep in mind that the IVR factor of Eq. (3.3) is based on experimental data over a range of $\varepsilon$ and $E-EA$ up to about 0.2 eV only, such that differences between the VW and VW+IVR curves at $\varepsilon > 0.2$ eV may at least in part be artificial.[30–32]

The distribution functions $f(E,\varepsilon)$ of Fig. 3 can be further rationalized by separately inspecting the average energy $\langle\varepsilon\rangle$ of the emitted electrons and the shape of the reduced distribution functions $f(E,\varepsilon/\langle\varepsilon\rangle)$. We first illustrate $f(E,\varepsilon/\langle\varepsilon\rangle)$. Figure 4 shows the curves of Fig. 3 in this representation. Now the VW and VW+IVR curves nearly coincide and, apart from the maximum near $\varepsilon = 0$, the RRKM curve is also not too different from the VW and VW+IVR results. The shape of the curves can well be approximated by expressions of the type

$$f(E,\varepsilon/\langle\varepsilon\rangle) \propto (\varepsilon/\langle\varepsilon\rangle)^n \exp(-\varepsilon/\langle\varepsilon'\rangle). \tag{3.10}$$

Figure 4 includes such curves for $n = 0.15$, 0.5, and 1. Obviously the distribution with $n = 0.15$ is much closer to the modelling results, both for the VW and VW+IVR calculations, than the "thermal" distributions with $n = 0.5$ and 1. This is confirmed by experimental observations. For example, distributions with $n = 0.15$, 0.28, and 0.58 were observed for electron emission from $C_{10}^-$, $C_{15}^-$, and $C_{18}^-$ cluster anions, respectively.[33] One may deduce from this observation that the distribution approaches a more thermal shape when the cluster size increases. However, this effect may also be due to other factors such as different contributions from higher partial waves ($l > 0$). This aspect is elaborated in Part II of this work[34] which applies the present approach to larger carbon clusters with varying shapes. It should be noted that the interpretation of the experimental distributions in Ref. 33 was done in terms of orbiting transition state/phase space theory, see Ref. 4. This approach cannot be applied to $SF_6^-$ for at least two reasons: (i) for $SF_6^-$, with only $s$-wave attachment, there are considerable angular momentum constraints, and (ii) dynamical effects included through electron capture theory are neglected. Nevertheless, Eq. (3.10) provides fairly good fits to the distribution functions $f(\varepsilon,\langle\varepsilon\rangle)$ calculated here, although the differences between treatments omitting and including electron capture theory (curves a and b in Fig. 4) are not negligible and Eq. (3.10) does not exactly reproduce the calculated full distribution $f(\varepsilon,\langle\varepsilon\rangle)$.

As the various dynamical factors do not strongly influence the shape of $f(\varepsilon,\langle\varepsilon\rangle)$, it appears more meaningful to focus attention on the average energy $\langle\varepsilon\rangle$. The simplicity of Eqs. (3.1)–(3.3), (3.6), (3.7), (3.8a), (3.8b), (3.8c), and (3.8d) allows one to do this analysis with only little computational effort. Figure 5 shows the dependence of $\langle\varepsilon\rangle$ on $E$ and on the applied model. Although the general trend of the three curves, i.e., an increase in $\langle\varepsilon\rangle$ with increasing $E$ is the same, there are considerable differences of $\langle\varepsilon\rangle$ for a given $E$. The VW results are always above the RRKM-type results. The VW+IVR results increasingly fall below the VW results. However, as the IVR factor of Eq. (3.3) was only derived from experiments over a range up to about 0.2 eV, this may at least, in part, be due to the limited energy range over which the IVR factor was derived. Therefore, the VW curve may be more realistic over large energy ranges. One should note again that experimental attachment cross sections at higher energies differ from the VW expression due to the VEX contributions. However, the latter should not be included in detachment treatments in as far as metastable anion states are concerned. For the curves a and b, $\langle\varepsilon\rangle$ is roughly about one-tenth of $E$. In the following this result is compared with finite heat bath and effective temperature concepts, remembering that $\langle\varepsilon\rangle/k$ generally is assumed[7] to be close to the effective daughter neutral temperature $T_d$ ($k$ denotes Boltzmann's constant).

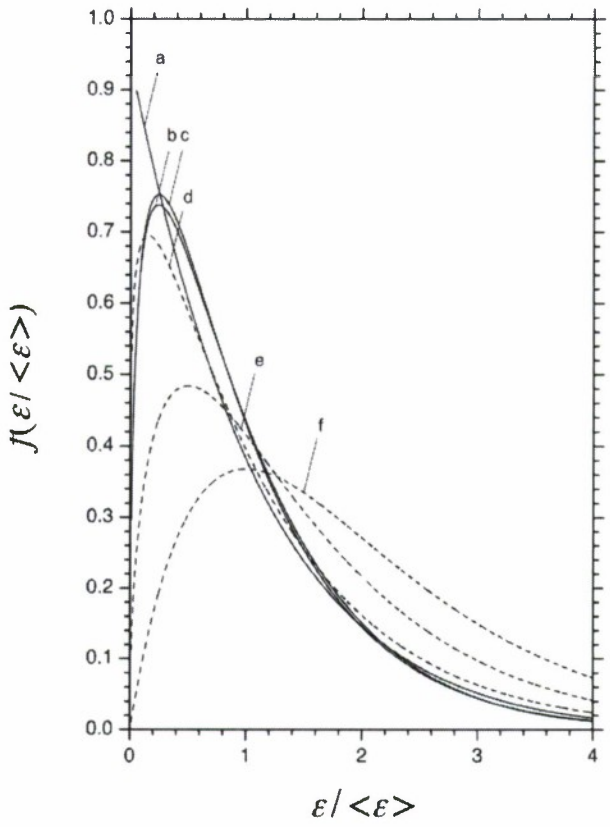


FIG. 4. Energy distribution $f(E,\varepsilon\langle\varepsilon\rangle)$ of electrons from the detachment from $SF_6^-$ ($E-EA=1$ eV); full curves=detailed calculations: (a) RRKM-type model with $\langle\varepsilon\rangle=0.0937$ eV, (b) electron capture VW-model with $\langle\varepsilon\rangle=0.109$ eV, and (c) VW+IVR-model with $\langle\varepsilon\rangle=0.0730$ eV; dashed curves=model functions (3.10) with exponents $n=0.15$ (d), 0.5 (e), and 1.0 (f).

## IV. EFFECTIVE TEMPERATURES

Our detailed calculations of detachment rate constants $k_{det}(E)$, electron energy distributions $f(E,\varepsilon)$, and their average $\langle\varepsilon(E)\rangle$ allow us to analyze the appropriateness of finite heat bath concepts and the accuracy of thermionic emission models. As similarly detailed experiments are not available, we do this analysis with our calculations for RRKM-type, VW, and VW+IVR models.

We first consider specific rate constants $k_{det}(E)$ and we ask whether $k_{det}(E)$ and $k_{det,\infty}(T)$ approached each other when $E$ and $T$ are related through Eq. (1.1). $k_{det,\infty}(T)$, i.e., the high pressure limiting rate constant of the falloff curve of detachment and attachment[15] has been measured in Ref. 19 and exploited to derive the improved value of the EA $=1.20(\pm0.05)$ eV. $k_{det,\infty}(T)$, $k_{det}(E)$, and attachment rate constants and cross sections in Ref. 15 were determined in an internally consistent manner. For the optimum experimental temperature, $k_{det,\infty}(650\text{ K})=115\text{ s}^{-1}$ was measured in Ref. 19. The average energy, $\langle E(650\text{ K})\rangle$, at this temperature is approximately 0.4 eV. At this energy obviously one has $k_{det}(E=0.4\text{ eV})=0$. [On the other hand, $k_{det}(E=EA+0.4\text{ eV})\approx10^6\text{ s}^{-1}$.] A microcanonical internal energy distribution just does not provide energies which are high enough to overcome the threshold energy EA=1.2 eV. The finite heat bath concept of Eq. (1.1) in this respect does not apply to detachment rates.

We next consider parent reactants $SF_6^{-*}$ directly at the moment before electron emission takes place. The energy $E$ then already has been used to overcome EA and the remainder $E-EA$ is partitioned between the daughter neutral $SF_6$ and the electrons. The energy distribution $f(E,\varepsilon)$ calculated in Sec. III through energy conservation is complementary to the energy distribution of the daughter neutral, and, on average, one has

$$E-\text{EA}=\langle E_d\rangle+\langle\varepsilon\rangle, \tag{4.1}$$

where $\langle E_d\rangle$ is the average internal energy of the daughter neutral. Identifying $\langle E_d\rangle$ with the average thermal internal energy of a canonical distribution of $SF_6$, Eq. (4.1) allows one to define an effective temperature $T_d(E)$ of the daughter neutral. (It is common practice to neglect $\langle\varepsilon\rangle$ against $\langle E_d\rangle$.) Then, $T_d$ follows from Eq. (4.1) with $\langle E_d\rangle$ obtained from the thermodynamic relation

$$\langle E_d\rangle=\sum_{j=1}^{s}h\nu_j[\exp(h\nu_j/kT_d)-1]^{-1}, \tag{4.2}$$

with the $s=15$ frequencies $\nu_j$ of $SF_6$. Often, however, $T_d$ is not derived from Eq. (4.2), but from the daughter vibrational density of states $\rho_d(E')$ through

$$kT_d=[d\ln\rho_d(E')/dE']^{-1}. \tag{4.3}$$

This simplification introduces inaccuracies, the latter because $\rho_d(E')$, such as obtained from Beyer–Swinehart counting,[4] is an irregular step function over the energy range of interest

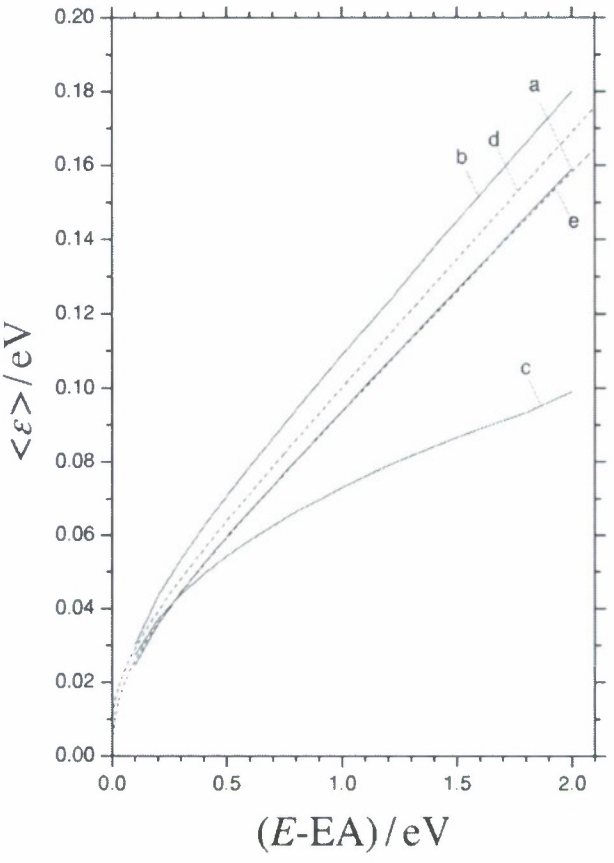


FIG. 5. Average energy $\langle\varepsilon\rangle$ of electrons detached from $SF_6^-$ at total energy $E$. Full curves=detailed calculations; (a) RRKM-type model; (b) electron capture VW-model; (c) electron capture with IVR=VW+IVR model. Dashed lines=thermionic emission results; (d) putting $\langle\varepsilon\rangle=0$ in Eq. (4.1); (e) including finite $\langle\varepsilon\rangle$ from Eqs. (4.1), (4.2), and (4.4); see text.

and needs appropriate and grain-dependent smoothing. We have avoided this practical problem by using the Whitten–Rabinovitch approximation of Eqs. (3.7), (3.8a), (3.8b), (3.8c), and (3.8d), see above.

$T_d(E)$ is the central quantity of the further analysis discussed here. One may ask whether finite heat bath arguments apply and allow one to obtain $\langle\varepsilon(E)\rangle$ from the relation

$$\langle\varepsilon(E)\rangle \approx kT_d(E). \tag{4.4}$$

In order to answer this question, Fig. 5 compares $\langle\varepsilon(E)\rangle$ from Eqs. (4.1), (4.2), and (4.4) with our detailed modeling results. One realizes that Eq. (4.4) with $kT_d(E)$ from Eqs. (4.1) and (4.2) [i.e., without the common assumption $\langle\varepsilon\rangle=0$ and without using Eq. (4.3)] gives nearly perfect agreement with the detailed results for the RRKM-type model (curves a and e in Fig. 5). On the other hand, neglecting $\langle\varepsilon\rangle$ in Eq. (4.1) leads to curve d in Fig. 5 which is between the results for the RRKM-type and VW models. The differences to the VW+IVR results (curve c in Fig. 5) are even larger. Although $\langle\varepsilon\rangle$ from the finite heat bath calculations with the purely thermodynamic value of $\langle E_{SF_6}(T_d)\rangle$ gives semiquantitative agreement with the detailed modeling results and certainly can be used for simple estimates, dynamical contributions to electron emission, such as specified by the RRKM-type, VW, and VW+IVR calculations, lead to deviations from Eq. (4.4). These are most pronounced for the VW+IVR model (which, however, may not be realistic for larger energies, see above).

$T_d(E)$ has also been used to express $k_{det}(E)$ in the simplified form,[6]

$$k_{det}(E) \approx \nu(E)\rho_d(E-\mathrm{EA})/\rho_p(E), \tag{4.5}$$

with densities of states $\rho_d(E')$ and $\rho_p(E')$ of the daughter neutral and the parent anion, respectively. $\nu(E)$ here is given by

$$\nu(E) = 2\mu[kT_d(E)]^2\sigma_c(E)/\pi^2\hbar^3 \tag{4.6}$$

and

$$\sigma_c(E) = \int_0^\infty \varepsilon\sigma_{at}(\varepsilon)\exp[-\varepsilon/kT_d(E)]d\varepsilon \Big/ \int_0^\infty \varepsilon\exp[-\varepsilon/kT_d(E)]d\varepsilon, \tag{4.7}$$

with the attachment cross section $\sigma_{at}(\varepsilon)$. We have explicitly calculated $\nu(E)$ using $T_d(E)$ and exploiting the relation

$$\varepsilon\sigma_{at}(\varepsilon) = P(E,\varepsilon)[kT_d(E)]^2/\pi\hbar, \tag{4.8}$$

see Secs. II and III. Using the (slightly corrected, see above) Whitten–Rabinovitch approximation for $\rho_d(E')$ and $\rho_p(E')$ in Eq. (4.5) then leads to the results which in Fig. 6 are compared with the original $k_{det}(E)$. There are differences of about

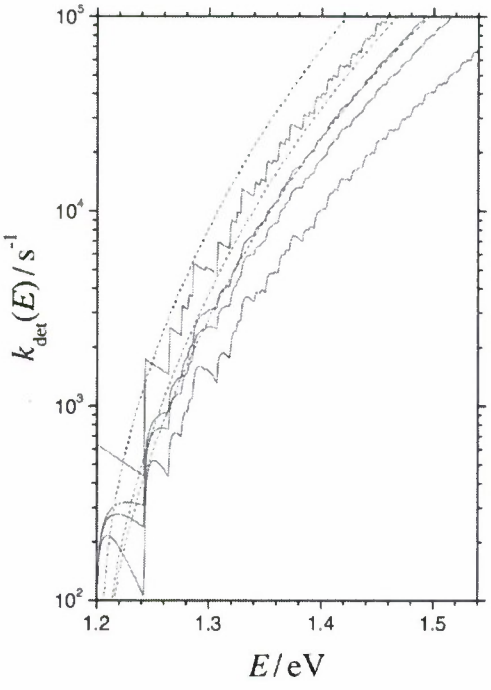


FIG. 6. Specific rate constants $k_{det}(E)$ for electron detachment from $SF_6^-$ [full curves: Detailed calculations identified in Fig. 2; dashed curves: Simplified thermionic emission approximations to the upper three detailed cases: The highest dashed curve is from Eqs. (4.5)–(4.8), the next uses (slightly corrected) Whitten–Rabinovitch densities of states for $\rho_d$, and the lowest curve uses $T_d$ from Eqs. (4.1), (4.2), and (4.4), see text].

a factor of 1.5, regardless which of the RRKM-type, VW, or VW+IVR models for $P(\varepsilon)$ is preferred. As Eq. (3.9) gives better accuracy and is simpler to use than the detour via Eqs. (4.5)–(4.7) and employing $T_d(E)$, we do not see advantages for using Eq. (4.5) for the present system. Instead of Eq. (4.8), often experimental nondissociative attachment cross sections have been used in Eq. (4.7). In the presence of VEX, then detailed balancing may have been violated, see above.

Apart from $T_d(E)$ there is still another effective temperature in use, an "isokinetic electron emission temperature" $T_e(E)$. This is defined through the equation

$$k_{det}(E) = \nu(E)\exp[-\mathrm{EA}/kT_e(E)]. \tag{4.9}$$

Having determined $k_{det}(E)$ previously and taking $\nu(E)$ from Eqs. (4.6) and (4.7), one derives $T_e(E)$ from Eq. (4.9). The results are shown in Fig. 7 together with $T_d(E)$ based on Eq. (4.1). The effective temperatures $T_d(E)$ and $T_e(E)$ defined above in Ref. 21 have been calculated for the present system as well. The results for $T_d(E)$ on the basis of Eq. (4.3) markedly differ from the results shown in Fig. 7 (about a factor of 2 at $E-\mathrm{EA}=0.05$ eV, a factor of 0.8 at $E-\mathrm{EA}=0.5$ eV). In contrast to this, the results for $T_e(E)$ (for $\mathrm{EA}=1.2$ eV) are accidentally in reasonable agreement.

If $\rho_d(E')$ and $\rho_p(E')$ were similar functions, $E$ and EA were not too distant, and the heat capacities $C_d$ defined by

$$C_d = d\langle E_d(T_d)\rangle/dT_d \tag{4.10}$$

were constant, then an approximate relation between $T_e(E)$ and $T_d(E)$ could be derived. According to Refs. 6 and 9, one would obtain

$$T_{e,\mathrm{app}}(E) \approx T_d(E) - \mathrm{EA}/2C_d(E) - \mathrm{EA}^2/12C_d^2(E)T_d(E). \tag{4.11}$$

The evaluation of Eq. (4.11) for the present system, however, gives incorrect results. For example, $T_{e,\mathrm{app}}(E)/T_e(E)=0.41$, 0.049, −0.28, −0.79, and −2.15 would be obtained for $E-\mathrm{EA}=1.11$, 0.81, 0.63, 0.44, and 0.20 eV, respectively. This failure of Eq. (4.11) is easily understood; none of the conditions used in its derivation are valid in the present case. For example, the difference of the frequencies of $SF_6$ and $SF_6^-$ introduces an error of a factor of 580 into the ratio of $\rho_d$ and $\rho_p$ and the specific heat $C_p$ is not at all independent of $T_d(E)$. The effective temperature $T_e(E)$, therefore, does not appear to be a useful quantity for the present example.

The transition from sparse low- to quasicontinuous high-energy behavior should be expected to take place when the energy of the daughter neutral exceeds its zero point energy. For $SF_6$, the latter amounts to $E_z=0.583$ eV. In reality, however, the smoothing effect of electron capture theory in comparison to RRKM-type calculations of $k_{det}(E)$ reduces the maximum deviations from the smoothed curve to ±2% already at $E-\mathrm{EA}\approx E_z/2$, see Fig. 2. In contrast to this, the maximum fluctuations of $\rho_d(E=E_z)$ still amount to more than ±50%. This is reflected in large fluctuations of $\Delta F(E,\varepsilon_i)/\Delta\varepsilon$ such as illustrated (for smaller energies) in Fig. 1(d). In any case, transitions between low-energy and high-energy behavior take place when $E-\mathrm{EA}$ is roughly of the order of $E_z$.

We finally comment on the difference between the values for $\mathrm{EA}(SF_6)$, obtained from the third law analysis of measured thermal detachment and attachment rate constants[19] ($\mathrm{EA}=1.2$ eV) and from a fit to measured $SF_6^-$ lifetime distributions on the basis of thermionic emission

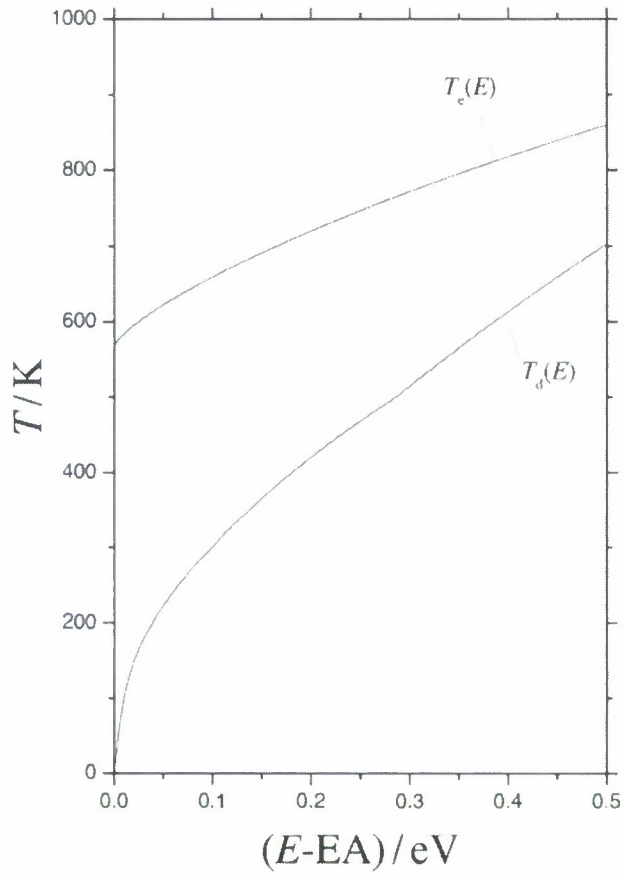


FIG. 7. Comparison of the daughter temperature $T_d(E)$, based on Eq. (4.1), and an effective or isokinetic temperature $T_e(E)$, from Eq. (4.9), in thermionic emission models of electron detachment from $SF_6^-$ (detailed calculations of this work, see text).

expressions[21] (EA=1.4 eV). The former approach employed the experimental attachment cross sections from Refs. 24 and 25 such that a comparison with $k_{det}(E)$ from the VW+IVR +VEX model should be made, see the lowest curve in Fig. 2. Employing EA=1.2 eV, in Ref. 21 a factor of five times higher values for $k_{det}(E)$ were derived than in the present work. A factor of 2 of this difference is due to the omission of one of the two electronic degeneracy factors [see Eq. (2.11) versus Eq. (4) from Ref. 21]. Another factor of about 1.5 is the consequence of using the simplified Eq. (4.5) instead of the original Eq. (2.1) for $k_{det}(E)$. This is illustrated by the differences of detailed and simplified results in Fig. 6. Furthermore, neither the experimental cross sections nor the VEX factor of Eq. (3.4) is expected to be valid over large energy ranges, apart from the fact that experimentally observed attachment cross sections and $k_{det}(E)$ most probably do not correspond to reverse rate processes. Experimental attachment cross sections and calculations with the VW +IVR+VEX model then both should not be used for calculations of $k_{det}(E)$.

## V. CONCLUSIONS

The present application of thermionic electron emission concepts to the specific rate constants $k_{det}(E)$ and energy distributions $f(E,\varepsilon)$ of the detachment of electrons from $SF_6^-$ have provided insight into the accuracy of the currently used models. It is emphasized that attachment and detachment are only linked by detailed balancing when they correspond to truly reverse processes. The comparison with calculations from statistical rate calculations, combined with electron capture theory and accounting for kinetic complications, reveals considerable inadequacies of the simplifications used within current thermionic emission models, at least in their application to the considered $SF_6^-$ system.

The present work demonstrates that the detailed state-resolved calculation of $k_{det}(E)$ from Ref. 15 can considerably be simplified when (slightly corrected) Whitten–Rabinovitch expressions for the densities of states are used, see Eq. (3.9). However, the gain in simplicity is at the expense of losing the low-energy fine structure in $k_{det}(E)$. It is illustrated that continuous energy distributions of the form of Eq. (3.10), i.e.,

$$f(E,\varepsilon) \propto (\varepsilon/\langle\varepsilon\rangle)^n \exp(-\varepsilon/\langle\varepsilon\rangle)$$

are obtained which have a "nonthermal" shape; i.e., $n \approx 0.15$ is found which is markedly smaller than "thermal expectations" of $n \approx 0.5$ or 1. The average energy $\langle\varepsilon\rangle$ as a function of the total energy $E$ also shows dynamical (and kinetic) influences of the process.

Apart from the dynamical refinements, the relation between $\langle\varepsilon\rangle$ and $E$ in accord with the thermionic emission concept can be roughly estimated by Eqs. (4.1) and (4.4), i.e., by the relation

$$E - \mathrm{EA} \approx \langle E_{\mathrm{SF}_6}(T_d)\rangle + \langle \varepsilon \rangle, \tag{5.1}$$

where $\langle E_{\mathrm{SF}_6}(T_d)\rangle$ denotes the internal vibrational energy of $SF_6$ at a canonical temperature $T_d$ and $\langle \varepsilon \rangle \approx kT_d$. The dependence of $T_d$ on $E$ can easily be calculated through Eq. (5.1) which corrects the sometimes used practice of omitting the last term $kT_d$. The representation of $k_{\mathrm{del}}(E)$ in terms of $T_d(E)$ appears less useful, as the direct calculation of $k_{\mathrm{det}}(E)$ through Eq. (3.9) is easily done and avoids unnecessary simplifications which introduce errors. Equation (3.9) also assures the intrinsically consistent detailed balancing link to attachment properties. At least for the present system, the introduction of an "isokinetic" electron emission temperature $T_e(E)$ appears less useful because the simplified relation (4.11) between $T_e(E)$ and $T_d(E)$ in the present case was shown to lead to erroneous results. The effective temperature $T_e(E)$, therefore, does not appear to provide much insight into the details of the phenomenon. The temperature $T_d(E)$ from Eq. (5.1) arising from the thermionic emission concept instead appears more useful, although it misses the dynamical details of the processes. Nevertheless, it provides a direct, yet approximate, estimate of the average electron energy $\langle \varepsilon \rangle$. One should note, however, that the shape of the relative electron energy distribution $f(E, \varepsilon/\langle \varepsilon \rangle)$ markedly differs from expectations for thermal distributions.

## ACKNOWLEDGMENTS

This work was supported by the European Office of Aerospace Research and Development (Award No. FA8655-09-1-3001). One of the authors (T.M.M.) is under contract with Boston College. Continuing encouragement by M. Berman and technical assistance by A. I. Maergoiz are gratefully acknowledged.

## APPENDIX: MOLECULAR PARAMETERS

The calculations of this work employed the vibrational quanta (in $cm^{-1}$) for $SF_6$ and $SF_6^-$ from Ref. 22. They are given by 346(3), 519(3), 611(3), 655(2), 779(1), and 965(3) for $SF_6$, as well as 237(3), 336(3), 306(3), 447(2), 626(1), and 722(3) for $SF_6^-$, with degeneracies shown in parentheses.

[1] L. Brouwer, H. Hippler, L. Lindemann, and J. Troe, J. Phys. Chem. **89**, 4608 (1985).
[2] J. E. Dove, H. Hippler, J. Plaeh, and J. Troe, J. Chem. Phys. **81**, 1209 (1984).
[3] D. C. Astholz, L. Brouwer, and J. Troe, Ber. Bunsenges. Phys. Chem. **85**, 559 (1981).
[4] T. Baer and W. L. Hase, *Unimolecular Reaction Dynamics. Theory and Experiments* (Oxford University Press, New York/Oxford, 1996).
[5] J. Troe, V. G. Ushakov, and A. A. Viggiano, Z. Phys. Chem. **219**, 699 (2005).
[6] J. U. Andersen, E. Bonderup, and K. Hansen, J. Phys. B **35**, R1 (2002).
[7] V. Weisskopf, Phys. Rev. **52**, 295 (1937).
[8] C. E. Klots, J. Chem. Phys. **90**, 4470 (1989); **93**, 2513 (1990).
[9] J. U. Andersen, E. Bonderup, and K. Hansen, J. Chem. Phys. **114**, 6518 (2001).
[10] J. U. Andersen, E. Bonderup, K. Hansen, P. Hvelplund, B. Liu, U. V. Pedersen, and S. Tomita, Eur. Phys. J. D **24**, 191 (2003).
[11] E. I. Dashevskaya, I. Litvin, A. I. Maergoiz, E. E. Nikitin, and J. Troe, J. Chem. Phys. **118**, 7313 (2003).
[12] E. I. Dashevskaya, I. Litvin, E. E. Nikitin, and J. Troe, Phys. Chem. Chem. Phys. **10**, 1270 (2008).
[13] E. Vogt and G. H. Wannier, Phys. Rev. **95**, 1190 (1954).
[14] I. I. Fabrikant and H. Hotop, Phys. Rev. A **63**, 022706 (2001), I. I. Fabrikant, H. Hotop, and M. Allan, *ibid.* **71**, 022712 (2005).
[15] J. Troe, T. M. Miller, and A. A. Viggiano, J. Chem. Phys. **127**, 244303 (2007).
[16] J. Troe, T. M. Miller, and A. A. Viggiano, J. Chem. Phys. **127**, 244304 (2007).
[17] J. P. Gauyaeq and A. Herzenberg, J. Phys. B **17**, 1155 (1984).
[18] L. G. Gerehikov and G. F. Gribakin, Phys. Rev. A **77**, 042724 (2008).
[19] A. A. Viggiano, T. M. Miller, J. F. Friedman, and J. Troe, J. Chem. Phys. **127**, 244305 (2007).
[20] J. Rajput, L. Lammieh, and L. H. Andersen, Phys. Rev. Lett. **100**, 153001 (2008).
[21] L. H. Andersen, Phys. Rev. A **78**, 032512 (2008).
[22] G. L. Gutsev and R. J. Bartlett, Mol. Phys. **94**, 121 (1998).
[23] C. E. Klots, Chem. Phys. Lett. **38**, 61 (1976).
[24] D. Klar, M.-W. Ruf, and H. Hotop, Chem. Phys. Lett. **189**, 448 (1992); Aust. J. Phys. **45**, 263 (1992).
[25] A. Sehramm, J. M. Weber, J. Kreil, D. Klar, M.-W. Ruf, and H. Hotop, Phys. Rev. Lett. **81**, 778 (1998); H. Hotop, M.-W. Ruf, M. Allan, and I. I. Fabrikant, Adv. At., Mol., Opt. Phys. **49**, 85 (2003).
[26] L. G. Christophorou and J. K. Olthoff, J. Phys. Chem. Ref. Data **29**, 267 (2000).
[27] R. W. Crompton and G. N. Haddad, Aust. J. Phys. **36**, 15 (1983).
[28] Z. L. Petrovie and R. W. Crompton, J. Phys. B **18**, 2777 (1985).
[29] T. Baer, Adv. Chem. Phys. **64**, 111 (1986).
[30] B. Baguenard, J. C. Pinaré, C. Bordas, and M. Broyer, Phys. Rev. A **63**, 023204 (2001).
[31] E. Surber and A. Sanov, J. Chem. Phys. **118**, 9192 (2003).
[32] F. Calvo, P. Parneix, and F. X. Gadéa, J. Phys. Chem. A **110**, 1561 (2006).
[33] F. Calvo, F. Lépine, B. Baguenard, F. Pagliarulo, B. Coneina, C. Bordas, and P. Parneix, J. Chem. Phys. **127**, 204312 (2007).
[34] J. Troe, T. M. Miller, and A. A. Viggiano, "On the accuracy of thermionic electron emission models. II. Eleetron detachment from $C_{60}^-$ and $C_{20}^-$" (unpublished).